European Review for Medical and Pharmacological Sciences 2022; 26: 1930-1938

Analysis of contrast-enhanced spectral chest CT optimal monochromatic imaging combined with ASIR and ASIR-V

J.-J. WANG[1], X.-T. CHI[2], W.-W. WANG[3], K. DENG[4]

[1]Department of Ultrasound, Jinan Maternity and Child Care Hospital Affiliated to Shandong First Medical University, Jinan, Shandong, P.R. China
[2]Department of Nuclear Medicine, Central Hospital Affiliated to Shandong First Medical University, Jinan, Shandong, P.R. China
[3]Department of Medical Imaging, Shandong Provincial Hospital Affiliated to Shandong First Medical University, Jinan, Shandong, P.R. China
[4]Department of Radiology, The First Affiliated Hospital of Shandong First Medical University & Shandong Provincial Qianfoshan Hospital, Jinan, Shandong, P.R. China

Jun-Jun Wang and Xiao-tong Chi contributed equally to this work

Abstract. – OBJECTIVE: The aim of the study was to explore the application of spectral chest CT optimal monochromatic imaging combined with ASIR and ASIR-V to optimize the image quality in the arterial phase.

PATIENTS AND METHODS: 62 patients who had undergone contrast-enhanced chest CT examination using spectral CT were included. Twelve sets of arterial phase images were acquired using GSI mode. The CNR, BHA values and subjective scores were statistically analysed. Thus, optimal monochromatic images were obtained. Then, the images were acquired by reconstruction using ASIR and ASIR-V at 30%, 50% and 70% levels. Six sets of images were obtained and compared with QC and the monochromatic image under FBP mode.

RESULTS: In FBP mode, the CNR of 80-keV images was 7.7±2.0, showing no significant difference with QC images ($p > 0.05$). The BHA value in the blood vessels was 45.2±23.1, which was lower than that in QC images ($p < 0.05$). The subjective image quality score of 80-keV images was 4.50±0.62. No significant difference was found in QC images ($p > 0.05$). The subjective score of the artefacts was 2.45±0.62, which was lower than that of QC images ($p < 0.05$). Thus, 80 keV was chosen as the optimal monochromatic energy to be reconstructed with ASIR and ASIR-V. The CNR of the 80keV+50% ASIR-V group was 13.9±4.3, which was higher than those of 140-kVp and 80-keV images in FBP ($p < 0.05$). The subjective score was 4.90±0.298, which was higher than that of other groups ($p < 0.05$).

CONCLUSIONS: Compared with conventional chest CT images in the arterial phase, 80keV+50% ASIR-V images can effectively eliminate beam-hardening artefacts and improve image quality.

Key Words:
Spectral CT, Image quality, Iterative reconstruction, Monochromatic imaging.

Introduction

Regarding the chest structure, the mediastinum, which comprises fat tissue, vessels, nerves, and lymph nodes, is intricate and susceptible to many diseases, including congenital dysplasia, inflammation, tumours, and vascular diseases. Due to the cardiovascular system, lesions in the mediastinum are hard to ignore. Moreover, the clinical symptoms of mediastinal lesions are uncharacteristic; thus, imaging examination has been validated as an important modality to diagnose mediastinal diseases. Contrast-enhanced CT has been widely used clinically due to its advantages of high-density resolution and ability to demonstrate the range, shape, density, blood supply and the surrounding tissues related to disease directly, features that are most beneficial for location determination and qualitative diagnosis[1,2]. With various limitations associated with other examinations, contrast-enhanced chest CT has become the preferred method to help diagnose mediastinal disease, although some limiting factors persist[3].

Contrast-enhanced chest CT is often used to assist in the detection and identification of various mediastinal diseases, such as the judgment of mediastinal tumours, invasion scope and efficacy evaluation of mediastinal lung cancer[4], identifica-

Corresponding Author: Kai Deng, MD; e-mail: 289954749@qq.com

tion of benign and malignant mediastinal lymph nodes[2], and detection of mediastinal large blood vessel diseases. During examination, different diseases show various degrees of enhancement in the arterial phase; hence, it is of great importance to improve the image quality and contrast ratio of the mediastinum by reducing image noise and the influence of artifacts for the diagnosis, treatment, and recovery of disease.

On the one hand, in the arterial phase, when the traditional polychromatic X-ray passes through the high-density contrast medium in the superior vena cava or brachiocephalic vein, beam-hardening artefacts will appear in surrounding tissues. On the other hand, high image noise and low-density resolution from traditional CT blur the mediastinal structure. Both imaging approaches hinder the assessment of the enhancement quality concerning mediastinal lesions and surrounding tissues; consequently, improvement is imperative.

More recently, the continuous innovation of spectral CT has been proven to be of high clinical value in the reduction of beam-hardening artefacts and improvement of the contrast ratio mainly by monochromatic imaging[5]. Additionally, compared with filtered back projection (FBP), spectral CT adopts new reconstruction techniques, adaptive statistical iterative reconstruction (ASIR) and adaptive statistical iterative reconstruction-V (ASIR-V), which can reduce noise, increase the contrast noise ratio and decrease the radiation dose remarkably[6,7].

Based on previous observations, we speculated that spectral CT monochromatic imaging combined with ASIR and ASIR-V could effectively remove beam-hardening artefacts and improve the imaging quality in the mediastinum. To the best of our knowledge, this topic has not yet been reported. The purpose of this study was to investigate the best compound mode to optimize the image quality in the arterial phase of contrast-enhanced chest CT.

Patients and Methods

Patient Population

The protocol for this retrospective study was approved by the institutional review board. From October 2017 to June 2019, 62 patients who underwent contrast-enhanced chest CT using spectral CT were included (38 men and 24 women). The age ranges from 33 to 72 years, with a mean age of 54±7.2 years. The exclusion criteria were as follows: (I) the presence of other beam-hardening artefacts caused by metal material in the mediastinal region; (II) a mediastinal structure with an evident mass not sufficiently clear to assess the image quality.

CT Scan Protocol

All examinations were carried out using a 64-row multi-detector CT system (Discovery CT 750 HD; GE Healthcare, Milwaukee, WI, USA). Detailed GSI parameters were set by the manufacturer and were as follows: tube voltage, fast kVp switching between 80 and 140 kVp (0.5 ms); tube current, 260 mAs; thickness, 5.00 mm; pitch, 1.375:1; rotation time, 0.8 s/rot; scanning field of view (FOV), apex to the bottom of the lung at the end of inspiration; and displayed FOV, 36×36 cm. The nonionic contrast media (Omnipaque 300 gI/100 mL; GE Healthcare, USA) at the dose of 1.2 mL/kg was injected into the right (n = 49) or left antecubital vein (n =13) using a power injector at a rate of 3.0 mL/s. Next, the vein was flushed with 20 mL of saline at a rate of 3.0 mL/s. The arterial and venous phases were obtained at 25 to 30 seconds and 60 to 75 seconds after the injection of the contrast medium.

The volumetric CT dose index (CTDIvol) produced using this scanning protocol was 7.37 mGy for the patient population in our study.

Image Reconstruction

The arterial phase images were transferred to an AW4.7 workstation (GE Volume Share 4 AW 4.7; GE Healthcare) for post-processing analysis using a dedicated software GSI Viewer. In total, eleven groups of 40- to 140-keV monochromatic images at an interval of 10 keV and one group of 140-kVp (QC) images were reconstructed with a 1.25-mm section thickness and 1.25-mm interval with the standard reconstruction kernel in FBP.

Through analysis of the QC images and monochromatic image quality, optimal monochromatic images could be obtained. The optimal monochromatic images were reconstructed again using ASIR (GE Healthcare) and the ASIR-V (GE Healthcare) at 30%, 50% and 70% percentage weight at slice thicknesses of 1.25 mm.

Objective Image Quality Analysis

Quantitative image analysis was conducted using a GSI viewer workstation by a radiological fellow with three years of experience.

Manually drawn elliptical regions of interest (ROIs) were placed on two artefact areas, soft tis-

sue at the entrance of the thorax (clavicular joint soft tissue or anterior chest wall muscle) and ascending aorta, which were marked as artefact area ROIs (ROIa and ROIb). At the same level, background fatty ROIs (ROI0) were selected at adipose tissue free of artefacts at the contralateral axilla. Additionally, the aorta ROIs (ROIc) were drawn on the aorta free of artefacts at the level of the aortic arch, the window of the main pulmonary artery and pulmonary artery trunk. At the same level, background muscular ROIs (ROI1) were selected at anterior chest wall muscle free of artefacts. Each group shared the same size and location for ROIs. The ROIs (range, 50-100 mm^2) were as large as possible depending on the artefact and uniformity of the density without including other structures.

Next, the attenuation values (CT value in Hounsfield units) and standard deviation (SD) were derived from the ROI measurements, and all the data were measured three times, from which the mean values were calculated to ensure consistency. The beam-hardening artefact (BHA) values in soft tissue and blood vessels were calculated. The equation is as follows: $BHAa= (SDa^2 -SD0^2)^{½}$; $BHAb=(SDb^2 -SD0^2)^{½}$. Thereafter, the contrast-to-noise ratios (CNRs) of the three different levels were acquired. The equation is as follows: CNR=(CTc-CT1)/SD0. The average CNR was regarded as the CNR of the image.

Subjective Image Quality Analysis

Two radiologists (with 8 and 3 years of experience in thoracic imaging, respectively) who were blinded to the imaging reconstruction method independently read and scored each image according to the diagnostic image quality and severity of the artefact of each case. Additionally, the final results were obtained by consensus. The diagnostic image quality was assessed on a 5-point scale made by Schueller-Weidekamm et al[8,9]:

1) no diagnosis possible: major image noise, vascular and soft tissue cannot be distinguished;
2) confidence in making diagnosis degraded: image noise that impedes diagnosis, unclear structure of the mediastinum and hilus of the lung, weak pulmonary arterial enhancement;
3) moderate but sufficient for diagnosis: moderate image noise, sufficient pulmonary arterial enhancement and structure of the mediastinum for the diagnosis;
4) good: image noise minor not influencing the diagnosis, good pulmonary arterial enhancement, clear structure of the mediastinum, vascular and soft tissue can be distinguished;
5) excellent: non-perceivable image noise, enabling excellent differentiation of even small structures, excellent pulmonary arterial enhancement.

The degree of the beam-hardening artefact refers to the CT image artefact's criterion[4], which was recommended by the "European guidelines on quality criteria for computed tomography"[5]:

1) absent;
2) present but not interfering with diagnosis;
3) present and interfering with diagnosis;
4) non-diagnostic.

Statistical Analysis

All the measurements were analysed using SPSS Statistics (version 24, IBM Corp., Armonk, NY, USA). The results of continuous data were displayed as $\bar{x}\pm s$. The differences in BHA and CNR between the QC and monochromatic images were compared using one-way ANOVA, and the Bonferroni method was used for intragroup comparison. Subjective scores were statistically analysed using the rank-sum test. Optimal monochromatic images with smaller artefacts and a higher image quality were obtained. The optimal monochromatic images were acquired by reconstruction with ASIR and ASIR-V at 30%, 50% and 70% levels. Additionally, six sets of images were compared with QC and the monochromatic image under the traditional reconstruction mode (FBP) using the same statistical methods as previously described.

Results

Monochromatic Image with FBP (Figure 1)

In objective image quality analysis, comparisons of the BHA and CNR between the QC and monochromatic images are shown in Table I. The soft tissue results indicate that the BHA of 40- to 60-keV monochromatic images were significantly higher than those of QC images ($p < 0.05$), and the BHA of 100- to 140-keV monochromatic images were significantly lower than those of QC images ($p < 0.05$). No significant difference was found between the 70- to 90-keV monochromatic images and QC images ($p > 0.05$). However, intragroup comparison showed that the BHA of 70-keV monochromatic images was significantly higher than those of 80-keV and 90-keV monochromatic image ($p < 0.05$). Additionally, in blood vessels, the results show that the BHA of 40- to 70-keV monochromatic images was significantly

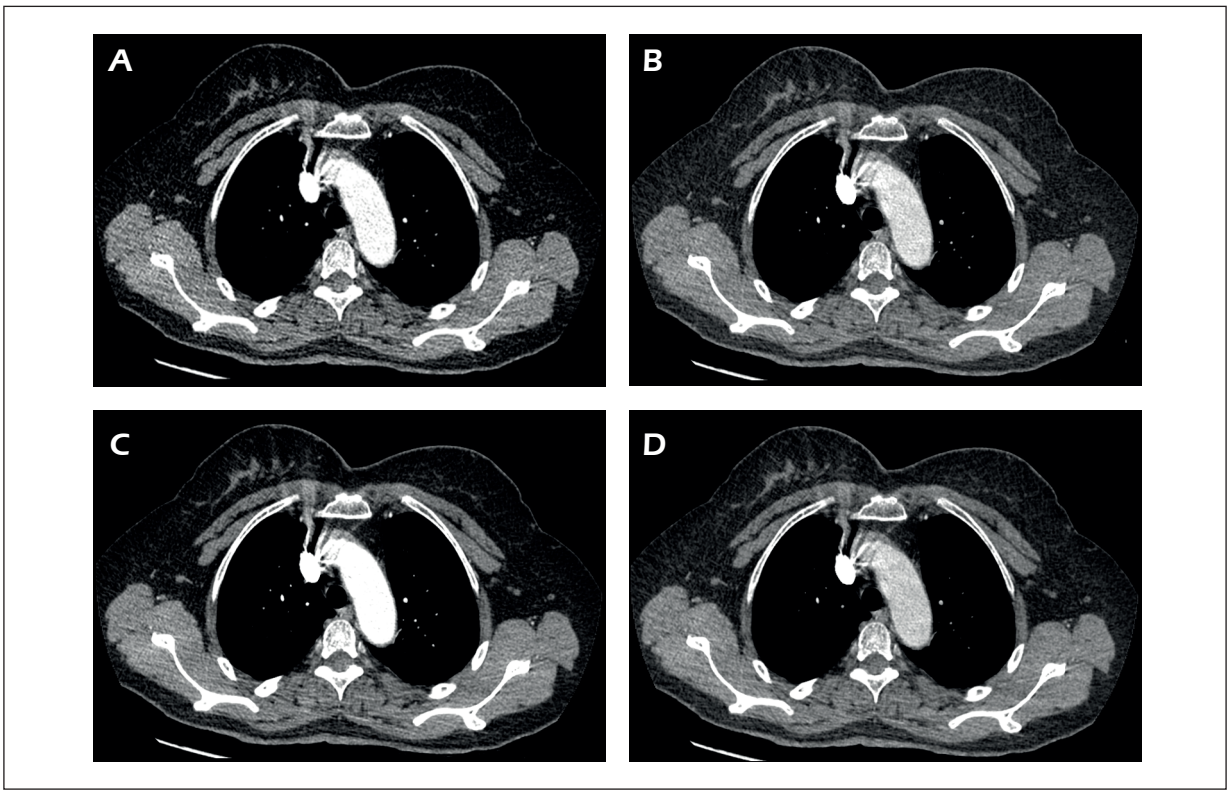

Figure 1. Monochromatic and QC Images with FBP mode demonstrated 80-keV images could effectively reduce the beam hardening artefacts while ensuring the image quality. **A**, QC image; **B**, 80kev image; **C**, 70kev image; **D**, 90kev image.

higher than that of QC images ($p < 0.05$), and the BHA of 80- to 140-keV monochromatic images were significantly lower than that of QC images ($p < 0.05$).

CNR analysis showed that the CNR of 40- to 70-keV monochromatic images was higher than that of QC images ($p < 0.05$). No significant difference was found between 80- to 100-keV monochromatic images and QC images ($p > 0.05$), but the CNR of the 80-keV images was higher than that of 90-keV and 100-keV images ($p < 0.05$). The CNR of 110- to 140-keV monochromatic images was significantly lower than that of QC images ($p < 0.05$).

In subjective image quality analysis (Table II), concerning the artefacts, the score of 40-keV to 70-keV images was higher than that of QC images ($p < 0.05$), an image quality level that is harmful. By contrast, the score of 80- to 140-keV images was significantly lower than that of QC images ($p < 0.05$), indicating the artefacts are reduced. Concerning the image quality, the scores of 40- to 60-keV and 90- to 140-keV images were lower than that of QC images ($p < 0.05$). However, the 70-keV image was higher ($p < 0.05$). Additionally, no significant difference was found in the image quality between the 80-keV images and QC images ($p > 0.05$).

To summarize, 80-keV images can effectively reduce the X-ray hardening artefacts while ensuring the image quality. Therefore, further research is warranted.

Monochromatic Image with ASIR and ASIR-V (Figure 2)

The 80-keV monochromatic images were chosen for reconstruction with ASIR and ASIR-V at 30%, 50% and 70% levels. Six sets of images were obtained and compared with QC images and 80-keV monochromatic images under the traditional reconstructed mode (FBP) with statistical analysis.

In the objective image quality analysis (Table III), 80 keV with 50% ASIR, 50% ASIR-V and 70% ASIR-V images showed significantly lower BHA values in both the soft tissue and blood vessels than the QC images with FBP; no significant difference was found between the other groups and QC images with FBP. Concerning the CNR analysis, compared with the QC images and

Table I. BHA and CNR between QC and monochromatic images with FBP mode.

Image	BHA		CNR
	Soft tissue	Blood vessel	
140kvp	49.8±26.6	52.3±23.6	8.8±3.6
40kev	143.5±86.2	161.5±78.6	12.6±3.7
50kev	96.6±58.0	109.5±53.1	11.2±3.4
60kev	70.2±39.3	79.9±35.8	12.8±4.3
70kev	55.3±29.4	63.5±29.4	10.0±3.5
80kev	43.4±20.8	45.2±23.1	7.7±2.0
90kev	34.1±19.2	37.4±17.8	5.8±2.0
100kev	28.6±16.5	31.7±15.2	5.5±1.7
110kev	25.7±14.5	27.7±13.4	4.3±1.5
120kev	23.7±13.2	25.0±12.2	3.4±1.4
130kev	22.4±12.3	22.8±11.3	2.7±1.3
140kev	21.4±11.6	20.4±22.4	2.1±1.2
F value	51.2	76.6	94.3
p-value	<0.05	<0.05	<0.05

80-keV images with FBP, any image with ASIR or ASIR-V was higher ($p < 0.05$), and with the same percent; the CNR of images with ASIR-V were significantly higher than that with ASIR ($p < 0.05$). Additionally, the CNR value of the reconstructed images increased with an increase in the IR level. Furthermore, in subjective image quality analysis (Table IV), the CNR of 80 keV+50% ASIR-V images were higher than that of other groups ($p < 0.05$).

Discussion

The contrast-enhanced chest CT has been extensively accepted in the qualitative diagnosis of chest diseases recently. However, in traditional contrast-enhanced chest CT, the beam-hardening artefacts in the mediastinum hinder the diagnosis of some lesions in the chest[10], particularly in the mediastinum, para-mediastinum and right hilar region. Additionally, the observation accuracy of the mediastinal structure was also severely impaired by the high image noise. We investigated whether combining GSI and ASIR or ASIR-V techniques could help to reduce the artefacts and decrease the image noise and obtain optimal CT images for the diagnostic performance of contrast-enhanced chest CT images. To our best knowledge, this is the first study to report this combination of techniques to reduce the beam-hardening artefacts, as well as improve the image quality.

Spectral CT can create a set of consistent energy information in a range of 40 to 140 keV using a fast-switching kilovoltage between 80 and 140 kVp X-rays within 0.5 ms. Thus, through projec-

Table II. The subjective scores between QC and monochromatic images with FBP mode.

Image	n	Artifact point			Image quality point		
		average	*Z* value	*p*-value	average	*Z* value	*p*-value
140kvp	62	2.71±0.71	—	—	4.56±0.59	—	—
40kev	62	3.90±0.30	-8.444	<0.05	1.05±0.22	-10.365	<0.05
50kev	62	3.53±0.50	-6.106	<0.05	1.11±0.32	-10.245	<0.05
60kev	62	3.34±0.54	-4.951	<0.05	3.74±0.77	-5.785	<0.05
70kev	62	3.15±0.69	-2.365	<0.05	4.76±0.50	-2.106	<0.05
80kev	62	2.40±0.62	-2.413	<0.05	4.50±0.62	-0.579	<0.05
90kev	62	2.35±0.52	-2.885	<0.05	3.31±0.67	-7.940	<0.05
100kev	62	2.31±0.47	-3.307	<0.05	3.05±0.66	-8.699	<0.05
110kev	62	2.27±0.45	-3.632	<0.05	2.73±0.66	-9.346	<0.05
120kev	62	2.23±0.49	-3.910	<0.05	1.94±0.67	-9.804	<0.05
130kev	62	2.18±0.46	-4.411	<0.05	1.58±0.62	-9.873	<0.05
140kev	62	2.10±0.43	-5.161	<0.05	1.11±0.32	-10.245	<0.05

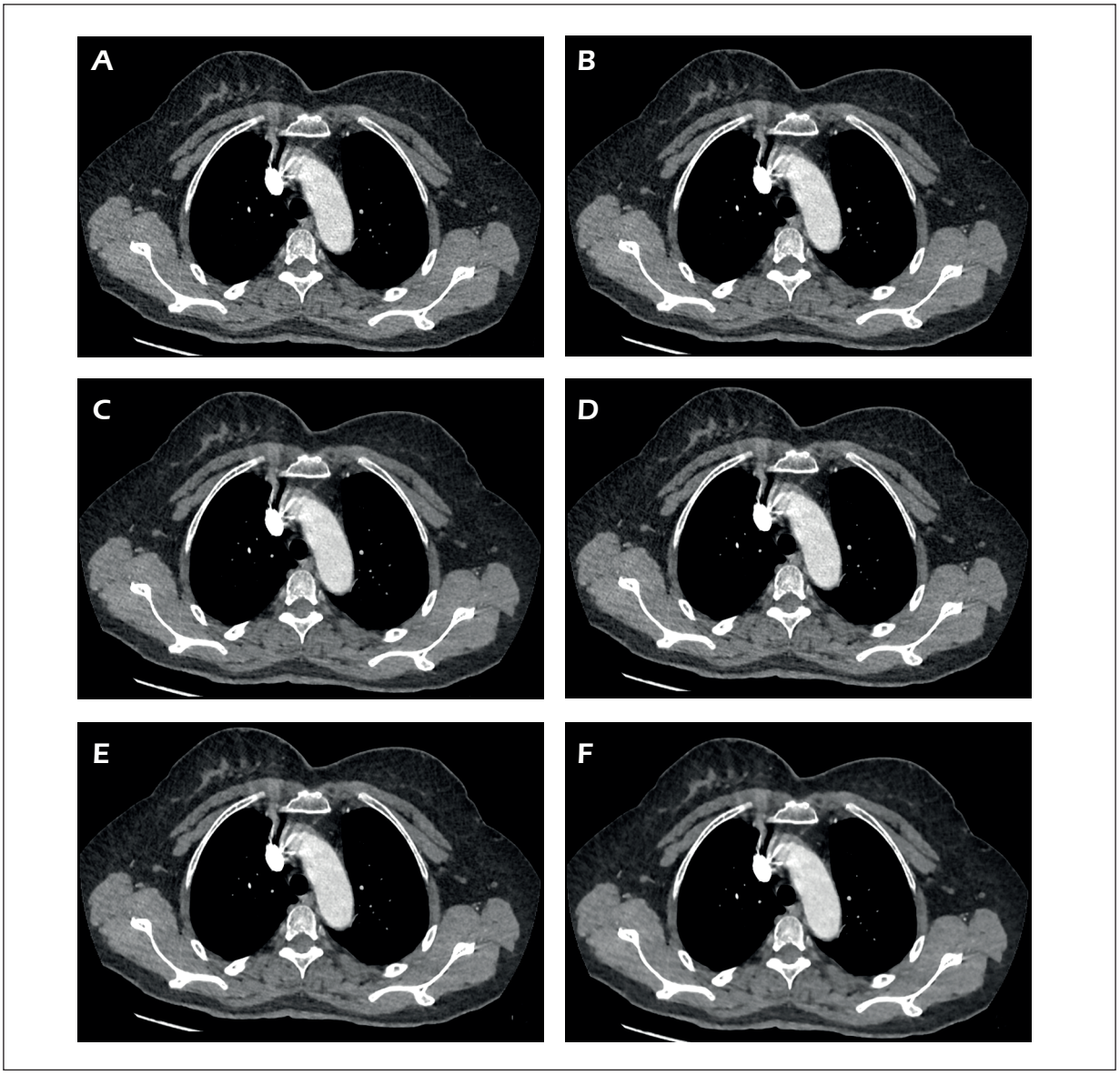

Figure 2. 80-keV monochromatic images with different levels of ASIR and ASIR-V demonstrated 80-keV monochromatic images combined with 50% ASIR-V not only improved the image quality but also reduced the beam hardening artefacts. **A**, ASIR30%+80kev image; **B**, ASIR-V30%+80kev image; **C**, ASIR50%+80kev image; **D**, ASIR-V50%+80kev image; **E**, ASIR70%+80kev image; **F**, ASIR-V70%+80kev image.

tion-based reconstruction, monochromatic images can reduce the beam-hardening effects by removing CT number shifts due to beam hardening[11]. Many previous studies[11-14] have demonstrated that higher quality monochromatic images were effective in reducing the beam-hardening artefacts and lower quality monochromatic images could help to improve the contrast ratio, both of which are beneficial to ameliorate the quality of the images. Thus, we can acquire optimal monochromatic images to eliminate the hardening artefacts produced by contrast agent and improve image quality, a finding that is more conducive to image diagnosis through comparative study.

Currently, filtered back projection (FBP) is the most used reconstruction algorithm to reduce beam-hardening artefacts by spectral CT. Additionally, the image in FBP not only shows evident noise but also tends to produce streak artefacts that lead to noisy images when lower doses are used[15]. An increasing number of new reconstruction algorithms have emerged to overcome FBP limitations, such as IRIS, ASIR, iDose, and AIDR. Among them, ASIR by GE, which in-

Table III. BHA and CNR between QC and monochromatic images with different reconstruction modes.

Image	BHA		CNR
	Soft tissue	Blood vessel	
140kvp+FBP	44.4±23.2	50.4±22.3	7.2±3.8
80kev+FBP	40.2±21.0	45.4±22.0	7.7±2.0
80kev+ASIR 30%	38.8±23.0	43.5±21.2	9.3±2.7
80kev+ASIR-V 30%	37.5±22.9	42.7±21.8	10.4±3.1
80kev+ASIR 50%	36.2±23.0	40.5±20.9	10.7±3.3
80kev+ASIR-V 50%	33.5±23.1	38.3±21.8	13.9±4.3
80kev+ASIR 70%	33.7±22.9	37.7±20.5	12.7±4.3
80kev+ASIR-V 70%	32.0±23.2	38.0±21.7	16.5±6.2
F value	1.416	0.856	25.734
p-value	>0.05	>0.05	<0.05

cludes a system noise model, can help maintain the spatial resolution of the image, reduce the image noise, and reduce the radiation dose by simulating the noise and assuming a noise difference between adjacent projections in the reconstruction process[16,17]. Prakash et al[17] reported a significant reduction in the radiation dose and increase in image quality in ASIR images compared with FBP images.

More recently, the new adaptive statistical iterative reconstruction (ASIR-V) is the latest released IR algorithm developed by GE. ASIR is unique and it incorporates multiple models for computation, focusing on system noise statistics, objects, and physical modelling[18]. Kwon et al[19] have shown that the more advanced noise modelling of ASIR-V provided higher noise reduction than ASIR, and the reconstruction of multiple models is significantly better than the single-model ASIR in reducing image noise, increasing density and spatial resolution, and reducing the radiation dose.

The objective results of this study found that, in the data of monochromatic images, increasing the photon energy level can lead to a decline in the image noise, BHA value and CNR. Compared with polychromatic images, 40- to 70-keV monochromatic images showed higher CNR and BHA values, indicating that, although the image contrast is higher, the large quantities of BHAs will hinder the diagnosis of some diseases around the superior vena cava. Conversely, 80- to 140-keV monochromatic images had lower BHA values and the less image noise, which are beneficial for image quality. However, the CNR values in 80- to 140-keV monochromatic images were decreased with the increase in the monochromatic level. This finding worsened the display of the mediastinal structure and should be ameliorated immediately.

Additionally, in the subjective results of this study, the 40- to 70-keV images had higher image quality, but the artefact level was higher, negatively affecting the diagnosis. The 80-keV image quality score was slightly lower than the 70-keV image quality score, but its artefact level was lower than that of QC and 70-keV images. Taken together, the data showed that 80-keV images can help to reduce the BHA and image noise, but no evident advantage was evident regarding the image contrast and spatial resolution. In a recent study, ASIR and ASIR-V were both proven to re-

Table IV. The subjective scores between QC and monochromatic images with different reconstruction modes.

Image	n	image quality point		
		average	*Z* value	*p*–value
140kvp+FBP	62	4.56±0.59	—	—
80kev+FBP	62	4.50±0.62	-0.579	>0.05
80kev+ASIR30%	62	4.66±0.542	-1.194	<0.05
80kev+ASIR-V30%	62	4.76±0.502	-1.323	<0.05
80kev+ASIR50%	62	4.84±0.413	-3.021	<0.05
80kev+ASIR-V50%	62	4.90±0.298	-3.406	<0.05
80kev+ASIR70%	62	3.55±0.645	-2.135	<0.05
80kev+ASIR-V70%	62	3.34±0.477	-2.687	<0.05

duce the image noise and improve the image quality[20-22]. ASIR and ASIR-V show significant effects in reducing image noise and improving image quality compared with traditional reconstruction algorithms. Therefore, 80-keV monochromatic images were combined with ASIR and ASIR-V to investigate whether they can effectively obtain optimal images with low image noise, low BHA and high-density resolution.

After evaluating the reconstruction images with ASIR and ASIR-V, the objective results revealed that combining ASIR and ASIR-V could lead to higher CNR values and better image quality than FBP reconstruction, without the advantage of reducing the BHA, consistent with previous research results. However, in contrast to the objective results, the subjective results showed that the score of the diagnostic image quality in 50% ASIR-V images was the highest. In subjective scoring, the 70% level of ASIR and ASIR-V reconstructed image scores were all less than 50% due to the low level of sharpness of the higher level of ASIR and ASIR-V reconstructed images, which would cause a "fuzzy" effect unlike that in previous CT images used for diagnosis, corroborating previous studies[18,22,23]. Dominik et al[24] also showed that images reconstructed with 70% ASIR-V have lower noise and higher spatial correlation, resulting in a "waxy" texture that is not familiar with traditional CT images recognized by radiologists, agreeing with our conclusions.

Therefore, in this study, which combined experimental statistics and actual clinical experience, the 80-keV single-energy images combined with ASIR-V 50% images are the best observation conditions. However, in the actual diagnosis process, if the local artefacts are too large, it is still necessary to combine the high-level single-energy images for a common diagnosis. For the radiation dose, the volumetric CT dose index (CTDIvol) of the monochromatic images selected in this study was 7.37 mGy. Additionally, 62 patients with conventional chest enhancement scan (120 kVp, automatic tube current) were selected, and their average CTDIvol value was 10.59±3.44 mGy. Using independent sample *t*-test, a statistically significant difference was found between the two groups ($p < 0.05$), and the radiation from spectral CT was reduced compared with that from the conventional scan; thus, the imaging approach can be used for clinical work.

The shortcomings of this study include the following: 1. The sample size was too small; 2. Only partial proportions of ASIR and ASIR-V were studied, and the image effects were not further compared in different proportions; 3. No detailed study is available concerning the comparison of factors such as contrast agent concentration and injection rate that may change the beam-hardening artefacts from the contrast agent; 4. This study only investigated the image quality of patients with clear mediastinal structures and no evident lesions. No further assessment of the beam-hardening artefacts in the lesion was performed. In future work, we will continue to improve relevant research.

Conclusions

80-keV monochromatic images combined with 50% ASIR-V in spectral CT not only ensures high image quality but also contributes to the reduction of contrast agent-hardening artefacts in the brachiocephalic vein and superior vena cava. The imaging approach may improve the accuracy of image diagnosis and can be routinely applied to contrast-enhanced chest CT examination.

Conflict of Interest

The authors declare that they have no conflicts of interest.

Acknowledgments

We are grateful to all the colleagues of CT Department in the First Affiliated Hospital of Shandong First Medical University.

References

1) Salonen O. CT characteristics of expansions in the middle and posterior mediastinum. Comput Radiol 1987; 11: 95-100.
2) Cascade PN, Gross BH, Kazerooni EA, Quint LE, Francis IR, Strawderman M, Korobkin M. Variability in the detection of enlarged mediastinal lymph nodes in staging lung cancer: a comparison of contrast-enhanced and unenhanced CT. AJR Am J Roentgenol 1998; 170: 927-931.
3) Carter BW, Betancourt SL, Benveniste MF. MR Imaging of Mediastinal Masses. Top Magn Reson Imaging 2017; 6: 153-165.
4) Wathen CG, Kerr KM, Reid W, Wightman AJ, Best JJ, Millar AM, Walker WS, Cameron EW, Douglas NJ. A comparison of cobalt (57Co) bleomycin scanning and contrast-enhanced CT scanning for assessment of the mediastinum in lung cancer. Chest 1999; 97: 1148-1151.
5) Mangold S, De Cecco CN, Schoepf UJ, Yamada RT, Varga-Szemes A, Stubenrauch AC, Caruso

D, Fuller SR, Vogl TJ, Nikolaou K, Todoran TM, Wichmann JL. A noise-optimized virtual monochromatic reconstruction algorithm improves stent visualization and diagnostic accuracy for detection of in-stent re-stenosis in lower extremity run-off CT angiography. Eur Radiol 2016; 26: 4380-4389.

6) Marin D, Nelson RC, Schindera ST, Richard S, Youngblood RS, Yoshizumi TT, Samei E. Low-tube-voltage, high-tube-current multidetector abdominal CT: improved image quality and decreased radiation dose with adaptive statistical iterative reconstruction algorithm--initial clinical experience. Radiology 2010; 254: 145-153.

7) Lim K, Kwon H, Cho J, Oh J, Yoon S, Kang M, Ha D, Lee J, Kang E. Initial phantom study comparing image quality in computed tomography using adaptive statistical iterative reconstruction and new adaptive statisticaliterative reconstruction v. J Comput Assist Tomogr 2015; 39: 443-448.

8) Schueller-Weidekamm C, Schaefer-Prokop CM, Weber M, Herold CJ, Prokop M. CT angiography of pulmonary arteries to detect pulmonary embolism: improvement of vascular enhancement with low kilovoltage settings. Radiology 2006; 241: 899-907.

9) Marin D, Choudhury KR, Gupta RT, Ho LM, Allen BC, Schindera ST, Colsher JG, Samei E, Nelson RC. Clinical impact of an adaptive statistical iterative reconstruction algorithm for detection of hypervascular liver tumours using a low tube voltage, high tube current MDCT technique. Eur Radiol 2013; 23: 3325-3335.

10) Kim C, Kim D, Lee KY, Kim H, Cha J, Choo JY, Cho PK. The Optimal Energy Level of Virtual Monochromatic Images From Spectral CT for Reducing Beam-Hardening Artifacts Due to Contrast Media in the Thorax. AJR Am J Roentgenol 2018; 211: 557-563.

11) Machida H, Tanaka I, Fukui R, Shen Y, Ishikawa T, Tate E, Ueno E. Dual-Energy Spectral CT: various clinical vascular applications. Radiographics 2016; 36: 1215-1232.

12) Rodriguez-Granillo GA, Carrascosa P, Cipriano S, De Zan M, Deviggiano A, Capunay C, Cury RC. Beam hardening artifact reduction using dual energy computed tomography: implications for myocardial perfusion studies. Cardiovasc Diagn Ther 2015; 5: 79-85.

13) Yoon JH, Chang W, Lee ES, Lee SM, Lee JM. Double low-dose dual-energy liver CT in patients at high-risk of HCC: a prospective, randomized, single-center study. Invest Radiol 2020; 55: 340-348.

14) Li X, Li Z, Li J, Song J, Yu Y, Liu B. Optimize non-contrast head CT imaging tasks using multiple virtual monochromatic image sets in dual-energy spectral CT. J Xray Sci Technol 2020; 28: 345-356.

15) Sagara Y, Hara AK, Pavlicek W, Silva AC, Paden RG, Wu Q. Abdominal CT: comparison of low-dose CT with adaptive statistical iterative reconstruction and routine-dose CT with filtered back projection in 53 patients. AJR Am J Roentgenol 2010; 195: 713-719.

16) Zhao L, Winklhofer S, Jiang R, Wang X, He W. Dual energy CT (DECT) monochromatic imaging: added value of adaptive statistical iterative reconstructions (ASIR) in portal venography. PLoS One 2016; 11: e0156830.

17) Prakash P, Kalra MK, Digumarthy SR, Hsieh J, Pien H, Singh S, Gilman MD, Shepard JA. Radiation dose reduction with chest computed tomography using adaptive statistical iterative reconstruction technique: initial experience. J Comput Assist Tomogr 2010; 34: 40-45.

18) De Marco P, Origgi D. New adaptive statistical iterative reconstruction ASiR-V:Assessment of noise performance in comparison to ASiR. J Appl Clin Med Phys 2018; 19: 275-286.

19) Kwon H, Cho J, Oh J, Kim D, Cho J, Kim S, Lee S, Lee J. The adaptive statistical iterative reconstruction-V technique for radiation dose reduction in abdominal CT: comparison with the adaptive statistical iterative reconstruction technique. Br J Radiol 2015; 88: 20150463.

20) Pontone G, Muscogiuri G, Andreini D, Guaricci AI, Guglielmo M, Baggiano A, Fazzari F, Mushtaq S, Conte E, Annoni A, Formenti A, Mancini E, Verdecchia M, Campari A, Martini C, Gatti M, Fusini L, Bonfanti L, Consiglio E, Rabbat MG, Bartorelli AL, Pepi M. Impact of a new adaptive statistical iterative reconstruction (ASIR)-V algorithm on image quality in coronary computed tomography angiography. Acad radiol 2018; 25: 1305-1313.

21) Wang W, Huang J, Wang A, Li Y, Peng J, Hu X, Liu Y, Zhang H, Li X. Dual-energy spectral computed tomography with adaptive statistical iterative reconstruction for improving image quality of portal venography. J Comput Assist Tomogr 2018; 42: 954-958.

22) Singh S, Kalra MK, Hsieh J, Licato PE, Do S, Pien HH, Blake MA. Abdominal CT: comparison of adaptive statistical iterative and filtered back projection reconstruction techniques. Radiology 2010; 257: 373-383.

23) Boedeker KL, McNitt-Gray MF. Application of the noise power spectrum in modern diagnostic MDCT: part II. Noise power spectra and signal to noise. Phys Med Biol 2007; 52: 4047-4061.

24) Benz DC, Gräni C, Mikulicic F, Vontobel J, Fuchs TA, Possner M, Clerc OF, Stehli J, Gaemperli O, Pazhenkottil AP, Buechel RR, Kaufmann PA. Adaptive statistical iterative reconstruction-V: impact on image quality in ultralow-dose coronary computed tomography angiography. J Comput Assist Tomogr 2016; 40: 958-963.